Journal of
Experimental
Botany
www.jxb.oxfordjournals.org

RESEARCH PAPER

PDMP induces rapid changes in vacuole morphology in *Arabidopsis* root cells

Falco Krüger[1,*], Melanie Krebs[1,*], Corrado Viotti[1], Markus Langhans[2], Karin Schumacher[1] and David G. Robinson[2,†]

[1] Department of Plant Developmental Biology, Centre for Organismal Studies, University of Heidelberg, Heidelberg, Germany
[2] Department of Plant Cell Biology, Centre for Organismal Studies, University of Heidelberg, Heidelberg, Germany

* These authors contributed equally to this manuscript.
† To whom correspondence should be addressed. E-mail: david.robinson@urz.uni-heidelberg.de

Abstract

PDMP (D-L-threo-1-phenyl-2-decanoyl amino-3-morpholino-1-propanol) is a well-known inhibitor of glucosylceramide synthase (GCS), a key enzyme in sphingolipid biosynthesis. Through the resultant increase in ceramides which interact with mTOR and Beclin1 (Atg6), this drug is also known to induce macroautophagy in mammalian cells. This study investigated the response of *Arabidopsis* root cells to PDMP, and what are probably numerous tightly packed small vacuoles in the control cells appear to fuse to form a single globular-shaped vacuole. However, during this fusion process, cytoplasm channels between the individual vacuoles become trapped in deep invaginations of the tonoplast. In both optical sections in the confocal laser scanning microscope and in ultrathin sections in the electron microscope, these invaginations have the appearance of cytoplasmic inclusions in the vacuole lumen. These changes in vacuole morphology are rapid (occurring within minutes after application of PDMP) and are independent of ongoing protein synthesis. The tonoplast invaginations remain visible for hours, but after 24h almost all disappear. Experiments designed to examine whether ceramide levels might be the cause of the PDMP effect have not proved conclusive. On the other hand, this study has been able to rule out the release of Ca^{2+} ions from intracellular stores as a contributing factor.

Introduction

PDMP (D-L-threo-1-phenyl-2-decanoyl amino-3-morpholino-1-propanol) is a well-known inhibitor of glucosylceramide synthase (GCS), a key enzyme in sphingolipid biosynthesis in mammalian cell (Vunnam and Radin, 1980; Futerman and Riezman, 2005). It has recently also been shown to be a potent inhibitor of GCS in higher plants leading to changes in Golgi morphology and a concomitant reduction in secretory activity (Melser *et al.*, 2010). These effects may be related to increased ceramide levels (Dai *et al.*, 2004; Daido *et al.*, 2004) or to the release of calcium ions from the endoplasmic reticulum (Kok *et al.*, 1998; Sprocati *et al.*, 2006). The

original intention of the present study of using PDMP was to exploit the possibility that PDMP would be of value in ongoing studies on multivesicular body biogenesis (Viotti *et al.*, 2010; Scheuring *et al.*, 2011). This was based on an electron micrograph in Melser *et al.* (2010) which intriguingly showed a multivesicular body apparently attached to the *trans*-Golgi network of a Golgi stack in a root cell from an *Arabidopsis* seedling that had been treated with 10 μM PDMP for 48 h. Although this observation could not be repeated, this study stumbled instead upon another effect of PDMP not previously reported in the plant literature.

This study shows that response to PDMP entails a rapid and dramatic reorganization of the vacuolar compartment leading to the formation of a single vacuole with a rounded-up appearance. In section (both optical in the confocal laser scanning microscope and in the electron microscope), these vacuoles were seen to contain numerous cytoplasmic droplets, resembling those which can be formed by starvation-induced macroautophagy under conditions where vacuolar degradation is impaired (Yoshimoto *et al.*, 2004). However, the present study eliminated macroautophagy as a cause for the PDMP effects on vacuole morphology, and vacuolar inclusions are in fact deep invaginations of the tonoplast. Nevertheless, the PDMP effect can be regarded as a protracted form of protrusion autophagy (Bassham *et al.*, 2006) since the invaginations eventually disappeared after many hours of exposure to PDMP. The possibility that calcium ions are responsible for the PDMP effects has also been ruled out. Although PDMP itself is a synthetic ceramide analogue, experiments designed to manipulate ceramide levels were not entirely conclusive, so that it is not certain whether ceramides are the agent of PDMP-induced changes in vacuole morphology.

Materials and methods

Plant materials and growth conditions

Arabidopsis thaliana ecotype Columbia-0 was stably transformed with VHA-a3-RFP (Brüx *et al.*, 2008) and VHA-a3-GFP (Dettmer *et al.*, 2006) according to standard procedures. Seedlings were grown on 1 × MS (1% sucrose with pH adjusted to 5.8 with KOH). Plates were solidified using 0.6% phyto agar. Agar and MS basal salt mixture were purchased from Duchefa. Seeds were surface sterilized with ethanol and stratified for 48 h at 4 °C. Seedlings were grown at 22 °C with a 16/8 light/dark cycle. For treatments with PDMP, FB1, and ceramides, 5-day-old seedlings were incubated at room temperature in 3 ml of liquid medium (half-strength MS medium, 0.5% sucrose, pH 5.8) supplemented with the indicated concentrations for the indicated time. PDMP (cat. no. BML-SL210-0010) was obtained from ENZO Life Sciences. FB1 (fumonisin B1 from *Fusarium moniliforme*, cat. no. F1147) and cycloheximide (CHX, cat. no. 01810) were obtained from Sigma-Aldrich. The lipophilic dye FM 4–64 (cat. no. T13320) was obtained from Invitrogen and concanamycin A (ConcA, cat. no. sc-202111) was bought from Santa Cruz Biotechnology. All previously listed chemicals were dissolved in DMSO. Both types of ceramides (hydroxy and non-hydroxy ceramides; cat. nos. 1323 and 1322) were purchased from Matreya, shipped through BIOTREND, and dissolved in a solution of DMSO/ethanol (1:1).

Confocal laser scanning microscopy

For imaging by confocal laser scanning microscopy (CLSM), a Leica TCS SP5 II confocal laser scanning microscope equipped with a Leica HCX PL APO lambda blue 63.0 × 1.20 WATER UV water immersion objective was used. GFP fluorophores were excited at 488 nm with a VIS-Argon laser; mRFP fluorophores and FM4-64 were excited at 561 nm with a VIS-DPSS 561 laser diode. Emission was detected with Leica Hybrid Detectors between 500 and 555 nm (for GFP) and between 615 and 676 nm (for mRFP and FM4-64); detection pinholes were set to 1 Airy Unit for each wavelength. For image acquisition, the scanning speed was 400 Hz with a line average of 5 and the image format was either 512 × 512 or 1024 × 1024 pixels. Z-stacks were recorded with a step-size of 420 nm. Post-processing of images and maximum projections of z-stacks were performed with the Leica Application Suite Advanced Fluorescence (LAS AF) software and Fiji (based on ImageJ 1.47b).

Calcium imaging using CLSM

FRET-based Ca^{2+} imaging was performed on a Leica SP5II system equipped with an inverted DMI6000 microscope stand, as described previously (Krebs *et al.*, 2012) with minor modifications. Images were recorded using a HCX PL APO lambda blue 63.0 × 1.20 WATER UV objective. For Ca^{2+} transient measurements, the resolution was set at 512 × 512 pixels, the pinhole to 2.69 Airy Units, scanning speed to 400 Hz, line average to 3, and an image was collected every 6 seconds. Enhanced cyan fluorescent protein (ECFP) was excited using the 458 nm laser line of the Argon laser. Fluorescence intensity values for ECFP (465–505 nm) and cpVenus (circular permutated Venus) (530–600 nm) were detected simultaneously in defined regions of interest. After background subtraction, the ECFP/cpVenus ratio was calculated followed by normalizing the ratio to the ratio value at time point zero (R_0). For imaging, the 5–7-day-old plate-grown *Arabidopsis* seedlings expressing NES-YC3.6 (yellow cameleon 3.6) were sandwiched between a cover slip and a nylon mesh (100 μm) in a custom-built perfusion chamber. To hold the seedlings in position, the sample–nylon mesh sandwich was slightly pressed against the cover slip by adding an open cover plate from the top. The sandwiched seedlings were immediately covered with 200 μl media (0.5 × MS, 1% sucrose, 10 mM MES-KOH with pH adjusted to 5.8) to prevent desiccation of the sample. Prior to measurement, seedlings were allowed to recover for approximately 15–30 min. Treatments were applied during imaging without interrupting image acquisition. At certain time points, different treatments (PDMP and/or ATP) were manually applied into the perfusion chamber. To achieve a rapid diffusion equilibrium of the substances the stock solutions (×2) were added in a 1:1 volume ratio to the bathing solution.

Chemical fixation for electron microscopy

Arabidopsis seedlings were fixed by immersion in 25 mM cacodylate (Caco) buffer (pH 7.2), containing 2% (v/v) glutaraldehyde and 10% (v/v) saturated picric acid, at 4 °C for 16 h (Ritzenthaler *et al.*, 2002). After four washes of 15 min each in 25 mM Caco buffer, seedlings were transferred to a secondary fixative containing 2% (w/v) osmium tetroxide and 0.5% (w/v) potassium ferrocyanide in 25 mM Caco buffer for 2 h at room temperature. Seedlings were washed twice in 25 mM Caco buffer and twice in distilled water before transferring to 2% (w/v) aqueous uranyl acetate for 16 h at 4 °C. After four washes in water, seedlings were dehydrated in acetone 30, 50, 70, and 90% in water and twice in acetone 100% for 15 min each at room temperature. Root tips were cut from the seedlings and submerged in 25, 50, and 75% Spurr's resin in acetone and than in 100% Spurr's for 45 min each at room temperature and finally transferred in fresh Spurr's 100% at 4 °C for 16 h. Samples were transferred in fresh Spurr's 100% for 4 h, and then placed in the oven at 60 °C for polymerization.

High-pressure freezing and freeze substitution for electron microscopy

Four- to five-day-old *Arabidopsis* root tips were excised from the seedlings, submerged in freezing media composed of 200 mM sucrose, 10 mM trehalose, and 10 mM Tris buffer (pH 6.6), transferred into planchettes (type 241 and 242, Wohlwend, Sennwald, Switzerland) and frozen in a high-pressure freezer (HPM010, Bal-Tec). Freeze substitution was performed in a electron microscope freeze substitution unit (EM AFS2, Leica) in dry acetone supplemented with 0.4% uranyl acetate at 85 °C for 16 h before gradually warming up to 60 °C over an 5-h period (Hillmer *et al.*, 2012). After washing with 100% ethanol for 60 min, the roots were infiltrated and embedded in Lowicryl HM20 at 60 °C (intermediate steps of 30, 50, and 70% in ethanol, 1 h each), and polymerized for 3 days with ultraviolet (UV) light in the freeze substitution apparatus. To improve sectioning quality, the blocks were then hardened with UV light for another 4 h at room temperature. Ultrathin sections were cut on a Leica Ultracut S, post-stained with aqueous uranyl acetate/lead citrate and examined in either Philips CM10 or JEM1400 (JEOL, Japan) transmission electron microscopes operating at 80 kV. Micrographs were recorded with a FastScan F214 digital camera (TVIPS, Germany).

Results

Effects of PDMP on the ultrastructure of Arabidopsis *root cells*

In a previous study, treatment of *Arabidopsis* roots with 10 µM PDMP for 48 h was reported to cause severe structural modifications in the Golgi apparatus (Melser *et al.*, 2010). These involved a 50% reduction in Golgi stack diameter and the accumulation of vesicles in the immediate vicinity of the stacks. This study could partially confirm the deleterious effects of PDMP on Golgi structure, especially when presented at a concentration of 50 µM for 2 h (Supplementary Fig. S1A, available at *JXB* online). However, exposure to 10 µM PDMP for the same duration had no visible effect on Golgi morphology (Supplementary Fig. S1B). In contrast, incubation with 10 µM PDMP for only 30 min induced dramatic changes in vacuole morphology. The effects of PDMP on vacuole morphology are essentially 2-fold and are best appreciated in root cells in a transgenic *Arabidopsis* line stably expressing the VHA-a3 isoform of the vacuolar ATPase fused to mRFP or GFP which locates to the tonoplast (Dettmer *et al.*, 2006; Brüx *et al.*, 2008). Firstly, instead of several pleiomorphic vacuoles per cell which is typical for control cells (Fig. 1A, C), PDMP-treated roots have only a single vacuole with a rounded-up appearance (Fig. 1 B, D). Secondly, numerous membrane-bound inclusions are visible in the lumen of the vacuole in PDMP-treated cells. In the electron microscope, these can be recognized as cytoplasmic droplets with a boundary membrane and contain diverse organelles (endoplasmic reticulum, mitochondria, plastids) in an undegraded condition (Fig. 1F, see also Fig. 3).

PDMP-induced vacuolar inclusions are formed rapidly and do not require ongoing protein synthesis

A time course experiment on VHA-a3-mRFP root cells was performed to determine how quickly the vacuole(s) reacted to PDMP. Astonishingly, vacuolar fusion and the formation of membrane-bound inclusions were visible within minutes of exposure to 10 µM PDMP (Fig. 2A–D). The presence of a single rounded-up vacuole was maintained even after prolonged exposure to 10 µM PDMP (Fig. 2E–G), although after 24 h only few inclusions remained visible (Fig. 2G). It is assumed that their loss was due to degradation. The cells chosen for these observations were subepidermal cortical cells in the region immediately behind the meristem. Cells higher up the root, moving into the elongation zone, were more vacuolate but also showed vacuolar inclusions (Fig. 2H, I). Roots of *Arabidopsis* which had been exposed to 30 µM cycloheximide for 30 min prior to the addition of PDMP also showed PDMP-induced vacuolar inclusions in (Fig. 2J, K). This indicates that the changes elicited by PDMP do not require continued protein synthesis.

PDMP-induced vacuolar inclusions are invaginations of the tonoplast

There are two possible explanations for the accumulation of cytoplasmic droplets in the lumen of the vacuole as a consequence of PDMP treatment. Firstly, as in macroautophagy, they could arise through the fusion of a double-membrane autophagosome with the tonoplast (Kwon and Park, 2008; Li and Vierstra, 2012). Under conditions where vacuolar pH is high due to treatment with the V-ATPase inhibitor ConcA, single-membrane autophagosomes (sometimes called autophagic bodies) remain undegraded within the vacuole for many hours (Yoshimoto *et al.*, 2004). Alternatively, they might arise either through the severance of transvacuolar strands or the entrapment of cytoplasmic channels between adjacent vacuoles as these vacuoles fuse to form a single vacuole.

To test for the possibility that the vacuolar inclusions induced by PDMP treatment were a result of macroautophagy, two types of experiment were performed. Firstly, 1 µM ConcA was applied to *Arabidopsis* roots for 30 min and then the roots were processed for electron microscopy. Under these conditions, structural modifications of the Golgi apparatus are induced (Viotti *et al.*, 2010; Scheuring *et al.*, 2011), but neither vacuolar inclusions nor changes in vacuole morphology were observed (Fig. 3A). A second approach was to see if PDMP could induce vacuolar inclusions in the roots of *Arabidopsis* mutants lacking different components of the core autophagy machinery. Three ATG mutant lines in which macroautophagy is either seriously impaired or cannot take place were used: *atg2-1* (Inoue *et al.*, 2006), *atg5-1* (Thompson *et al.*, 2005), and *atg7-2* (Hofius *et al.*, 2009). In all three cases, PDMP caused the formation of vacuolar inclusions (Fig. 3B–D).

Positive evidence that the vacuolar inclusions were in fact deeply penetrating invaginations of the tonoplast was obtained from thin sections cut from cryofixed root samples. These revealed direct continuities between the tonoplast and boundary membrane of the vacuolar inclusions even after 2 h of PDMP treatment (Fig. 4A). Further evidence came from an analysis of a z-stack series in root cells expressing VHA-a3-mRFP. As shown in Fig. 4B and C, individual inclusions which appear to be separated from the tonoplast have, in other optical levels, tubular connections to the tonoplast. In some cases, these may even traverse the vacuole (Fig. 4E, arrowheads). Perhaps even more convincing are the images obtained from an *Arabidopsis* line expressing the endoplasmic reticulum marker VMA21-GFP (Neubert *et al.*, 2008) together with the tonoplast marker VHA-a3-mRFP. With this line, this study was able to trace the penetration of the endoplasmic reticulum network into and along the invaginating tubules (Fig. 4D).

PDMP-induced tonoplast invaginations are relatively stable structures

In order to determine whether PDMP-induced tonoplast invaginations were being continually formed and severed, an FM4-64 uptake experiment was performed with the tonoplast marker VHA-a3-GFP. FM4-64 is a lipophilic styryl dye which is taken up via endocytosis and travels down the endocytic pathway to the tonoplast (Dettmer *et al.*, 2006). If the PDMP-induced vacuolar inclusions still remained connected
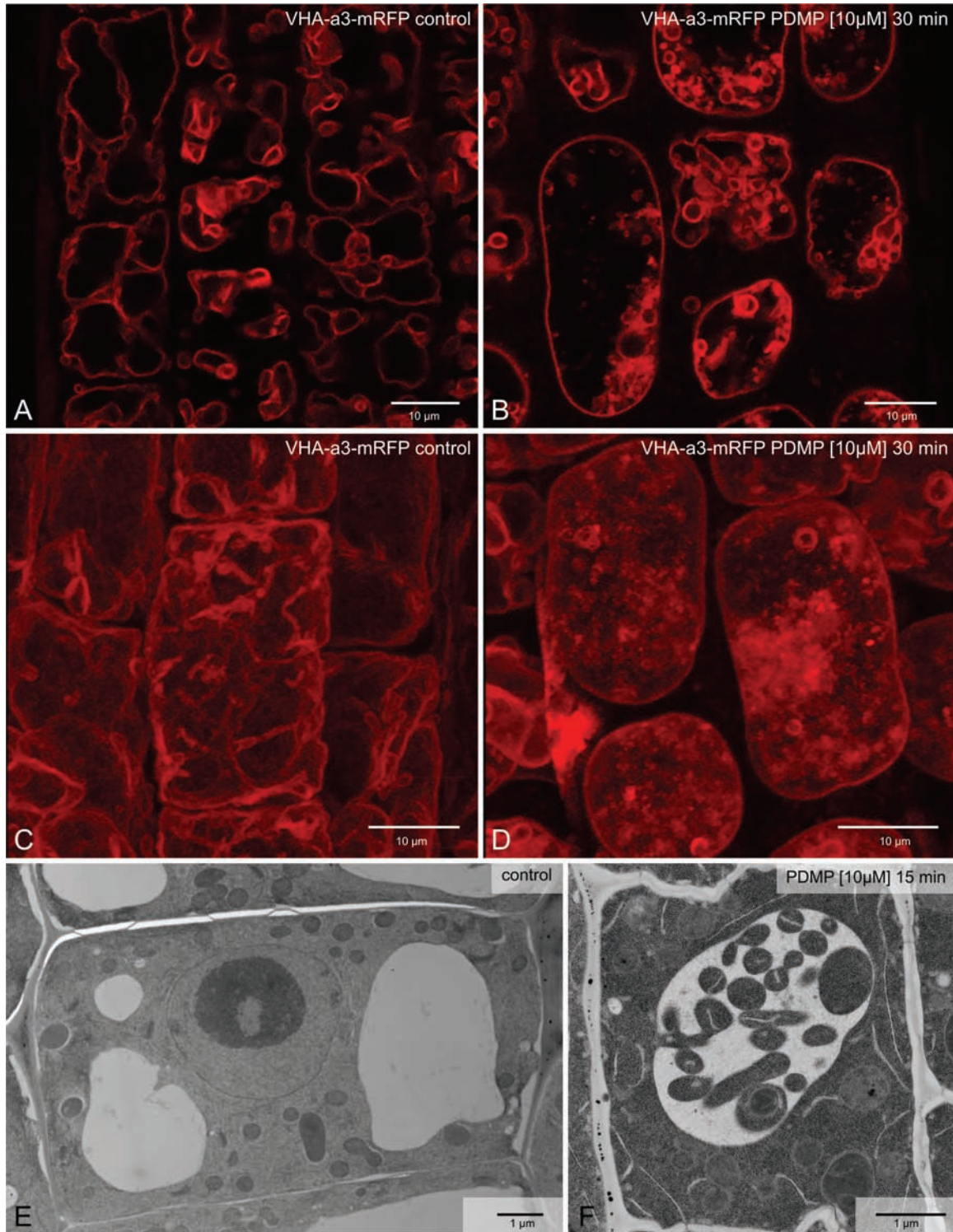
Fig. 1. PDMP effects on the vacuole of *Arabidopsis* root cells. (A, C, E) Control cells; (B, D, F) cells after 30 min exposure to 10 μM PDMP. (A–D) Tonoplast visualized by the presence of the fluorescent marker VHA-a3-mRFP: (A, B) single optical sections; (C, D) maximum projections of individual z-stacks. (E, F) High-pressure frozen cells. Bars, 10 μm (A–D) and 1 μm (E, F).

to the tonoplast, they would become stained with the dye after 1.5–2 h of staining. Lumenal membranes that do not become labelled with FM4-64 would then represent real inclusions that separated from the tonoplast before arrival of the dye. The results of a FM4-64 pulse-chase experiment are presented in Fig. 5. Roots were pre-treated with PDMP for 30 min followed by a 30-min pulse of FM4-64 (Fig. 5A, B). At this time point, the plasma membrane and endosomal membranes, but not the tonoplast, were labelled by FM4-64, and later, 105 min after starting the FM4-64 pulse,
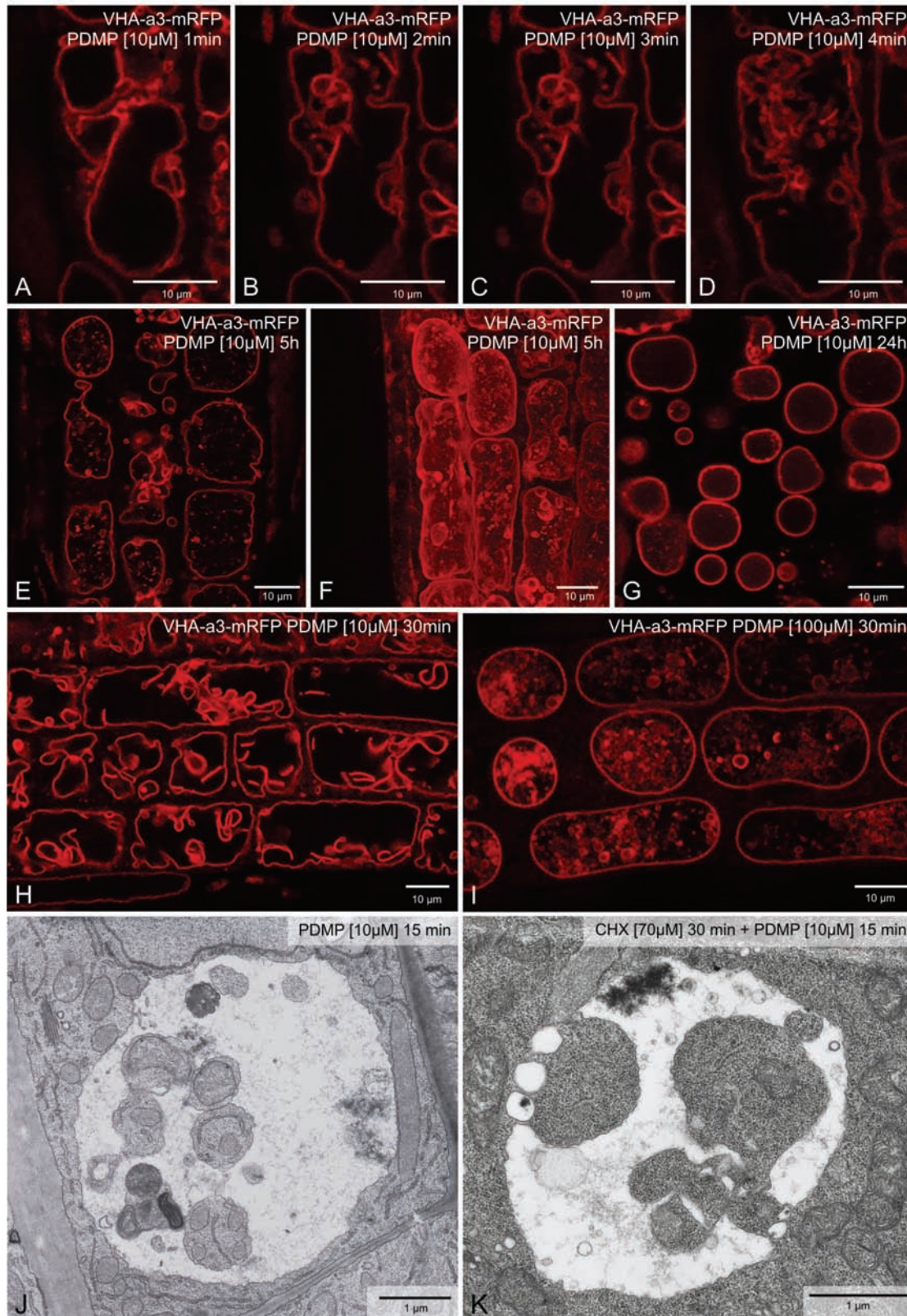
Fig. 2. PDMP effects are rapid and occur in the absence of protein synthesis. (A–D) Single root cell from a transgenic *Arabidopsis* plant expressing VHA-a3-mRFP over a 4-min period after addition of 10 µM PDMP. (E, F) Single optical section (E) and maximum projection (F) of cells after 5 h exposure to PDMP. (G) Single optical section after exposure to PDMP for 24 h: note the absence of vacuolar inclusions. (H, I) PDMP-induced [10 µM PDMP (H) or 100 µM PDMP (I)] vacuolar inclusions in cells near the elongation zone. (J, K) Chemically fixed *Arabidopsis* root cells after exposure to PDMP for 15 min: the roots in K were pretreated with 70 µM cycloheximide for 30 min prior to addition of 10 µM PDMP. Bars, 10 µm (A–I) and 1 µm (J, K).
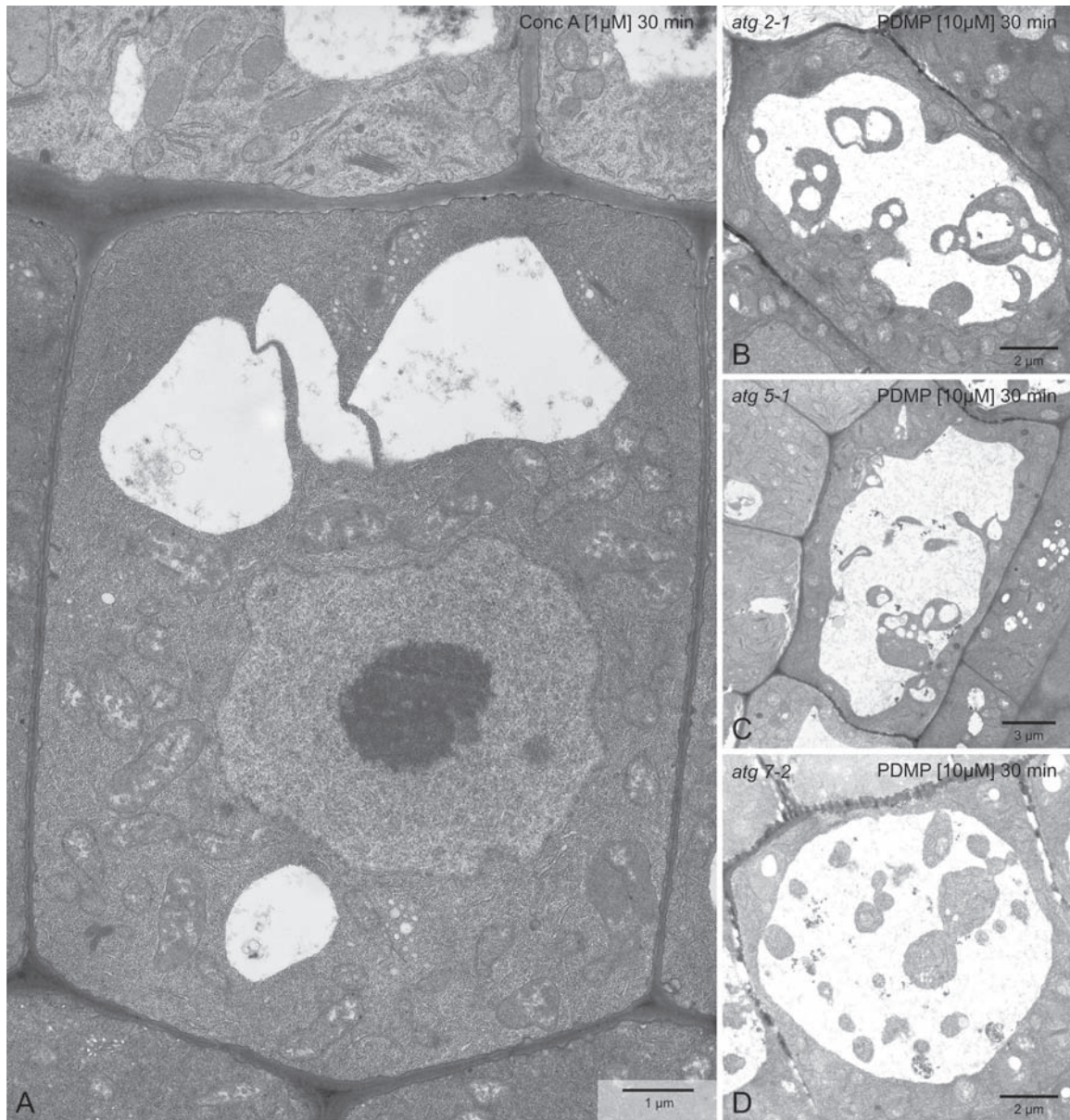
Fig. 3. PDMP-elicited vacuolar inclusions are not a result of macroautophagy. (A) Concanamycin A, which can induce vacuolar inclusions in N-starved *Arabidopsis* roots via macroautophagy, does not do so in short-term treatments of normal roots. (B–D In contrast, vacuolar inclusions can be observed in root cells of the autophagy mutants *atg2-1* (B), *atg5-1* (C), and *atg7-2* (D). Bars, 1 μm (A), 2 μm (B, D) and 3 μm (C).

a faint signal could be observed at the tonoplast (Fig. 5D). However, at this time point, not only had the dye reached the tonoplast, it had also labelled the membranes of almost all structures appearing inside the vacuolar lumen, indicating that these structures represent invaginations of the tonoplast. There were only rare cases when this study observed VHA-a3-GFP-labelled inclusions that were not stained with FM4-64 (Fig. 5C–E, arrowheads). This experiment demonstrates that the PDMP-induced membranous structures found inside the vacuolar lumen represent in most cases invaginations of the tonoplast. Moreover, these invaginations remained stable for at least 2 h and most likely were not being continually formed.

Is the effect of PDMP achieved by raised ceramide levels?

PDMP is a synthetic ceramide and competes with native ceramides in the formation of the GCS/UDP-glucose/ceramide complex (Asano, 2003). Its action therefore results in an elevation of cytosolic ceramide levels (Dai *et al.*, 2004; Daido *et al.*, 2004). In order to test whether the tonoplast invaginations induced by PDMP are a result of raised ceramide levels, this study followed two strategies. In the first case, ceramides were added exogenously in concentrations which have previously been successfully applied to *Arabidopsis* to induce programmed cell death (Liang *et al.*, 2003; Townley *et al.*,
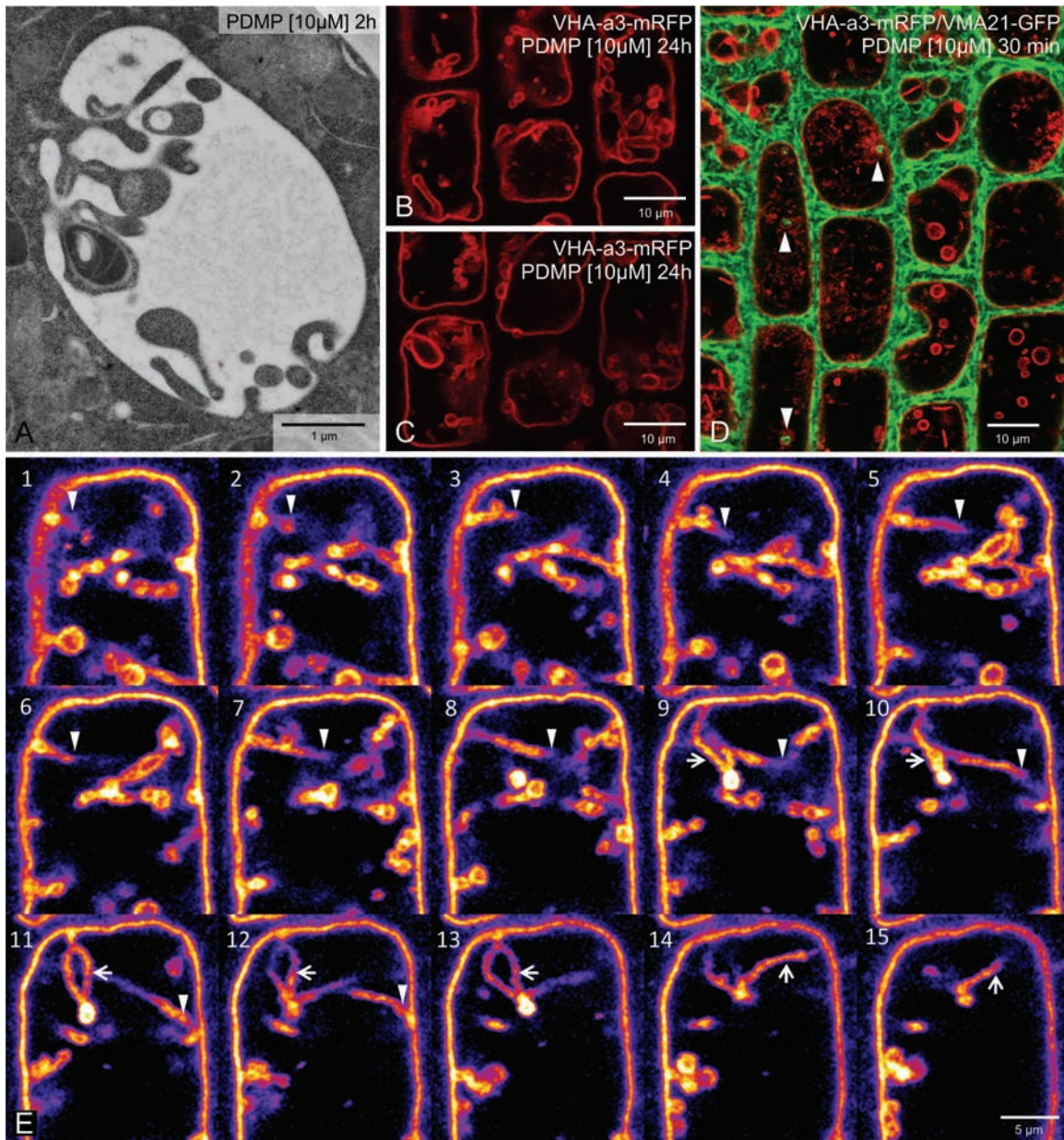
Fig. 4. PDMP-induced vacuolar inclusions are invaginations of the tonoplast. (A) Direct connections between the tonoplast and the boundary membrane of the vacuolar inclusions can be occasionally seen in cryofixed samples. (B, C) Two optical sections from a z-stack series taken of cells in an *Arabidopsis* root stably expressing the tonoplast marker VHA-a3-mRFP after 10μM PDMP treatment for 24 h: tubular invaginations penetrating deep into the lumen of the vacuole are seen in several cells. (D) The endoplasmic reticulum (labelled with VMA21-mRFP, red) can be seen to penetrate into the tubular invaginations (labelled with VHA-a3-GFP, green). (E) Single optical sections of a z-stack series taken from an *Arabidopsis* root tip cell expressing VHA-a3-mRFP: in order to emphasize the tubular invagination traversing the vacuole (arrowheads) as well as a tubular loop (arrows), the lookup table (LUT) was changed to 'fire' using the open source image processing software Fiji.

2005). In the second case, the inhibitor FB1, which inhibits the conversion of sphingosine to ceramides (Spassieva *et al.*, 2002; Guenther *et al.*, 2008), was applied in order to decrease ceramide levels prior to PDMP treatment. Again, inhibitor concentration and treatment times were chosen which have previously been shown to be effective in *Arabidopsis* roots (Markham *et al.*, 2011).

As shown in Fig. 6A–C, neither hydroxy- nor non-hydroxy-ceramides induced PDMP-like tonoplast invaginations. Instead, many cells showed a larger number of smaller rounded-up vacuoles. On the other hand, pretreatment with FB1 was effective in preventing the PDMP-induced formation of tonoplast invaginations (Fig. 6D, E). However, once again a tendency to form smaller vacuoles in cells in both the
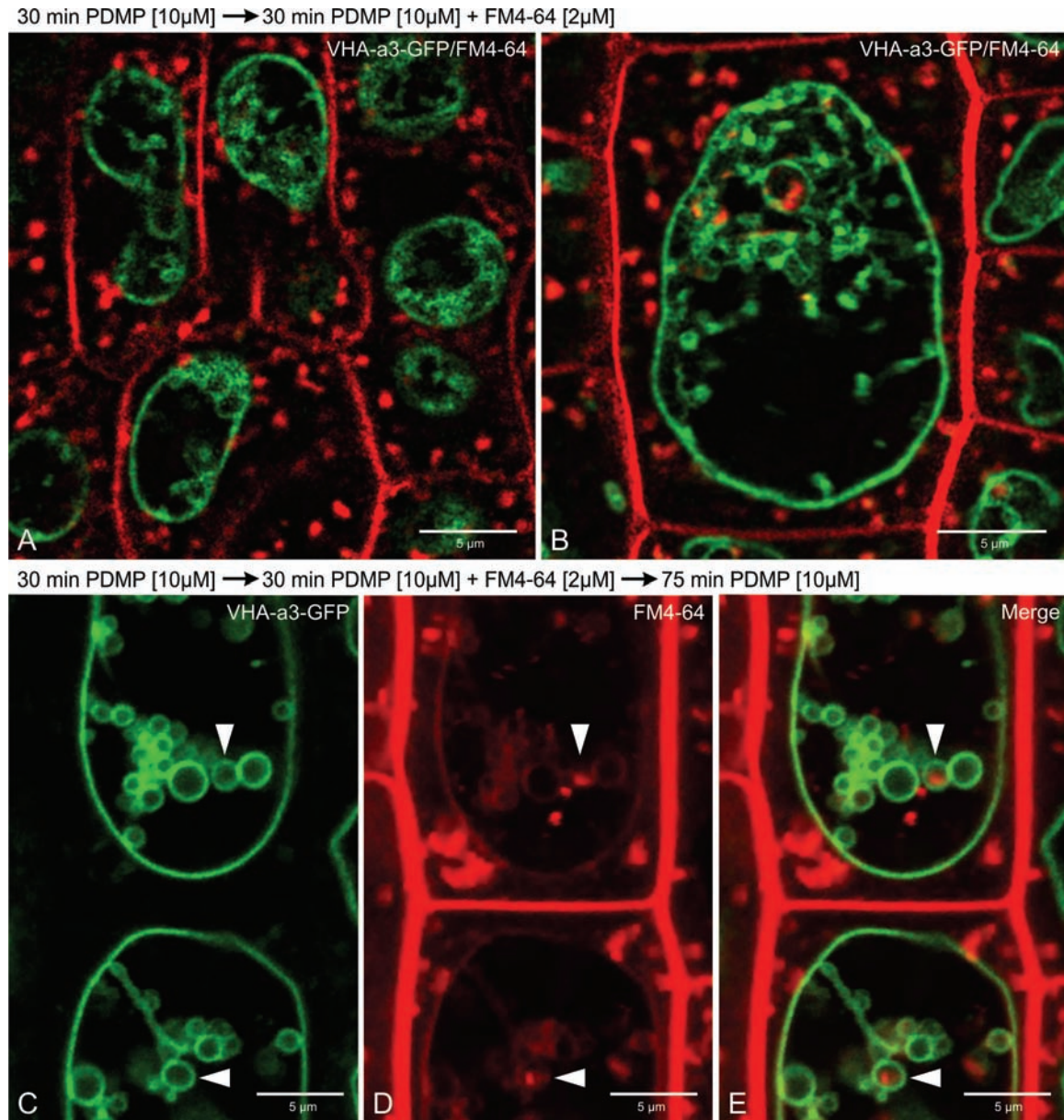
Fig. 5. PDMP-induced invaginations are stable structures. (A) Root cells from a stable transgenic *Arabidopsis* line expressing the tonoplast marker VHA-a3-GFP after incubation with 10 μM PDMP for 30 min, followed by a 30-min pulse with the endocytic tracer FM4-64: the tonoplast and endosomes are labelled by FM4-64, but the styryl dye has not yet reached the tonoplast. (B) One of the vacuolar inclusions has an internal red signal, indicating that a FM4-64 positive endosome has entered the tubular invagination. (C–E) Root cells as in A and B but after a further 75-min chase in PDMP medium without FM4-64: at this time FM4-64 has reached the tonoplast and the vacuolar inclusions (D) are also labelled with FM4-64, indicating that they are connected to the tonoplast; arrowheads point to VHA-a3-GFP labelled inclusions that were not stained with FM4-64. Bars, 5 μm.

root tip (Fig. 6D) and in the elongation zone (Fig. 6E) was discernible.

Only high concentrations (100 μM) of PDMP induce cytosolic Ca²⁺ transients in Arabidopsis *root cells*

Since PDMP has been reported to induce short-term changes in cytosolic Ca^{2+} homeostasis in kidney cell lines (Kok *et al.*, 1998), this study investigated whether PDMP was also able to stimulate transient increases in cytoplasmic Ca^{2+} in

Arabidopsis root cells. Live cell Ca^{2+} imaging was performed using stable transgenic *Arabidopsis* lines expressing the cytoplasmic Ca^{2+} sensor NES-YC3.6 (Krebs *et al.*, 2012). Cytosolic Ca^{2+} dynamics were recorded from cortical and epidermal cells within the root elongation zone of 5–7-day-old *Arabidopsis* seedlings. At certain time points, different treatments (DMSO, PDMP, or ATP) were applied to the seedlings (Fig. 7). To achieve a rapid diffusion equilibrium of the drug and control substances, the stock solutions were added in a 1:1 volume ratio to the bathing solution without
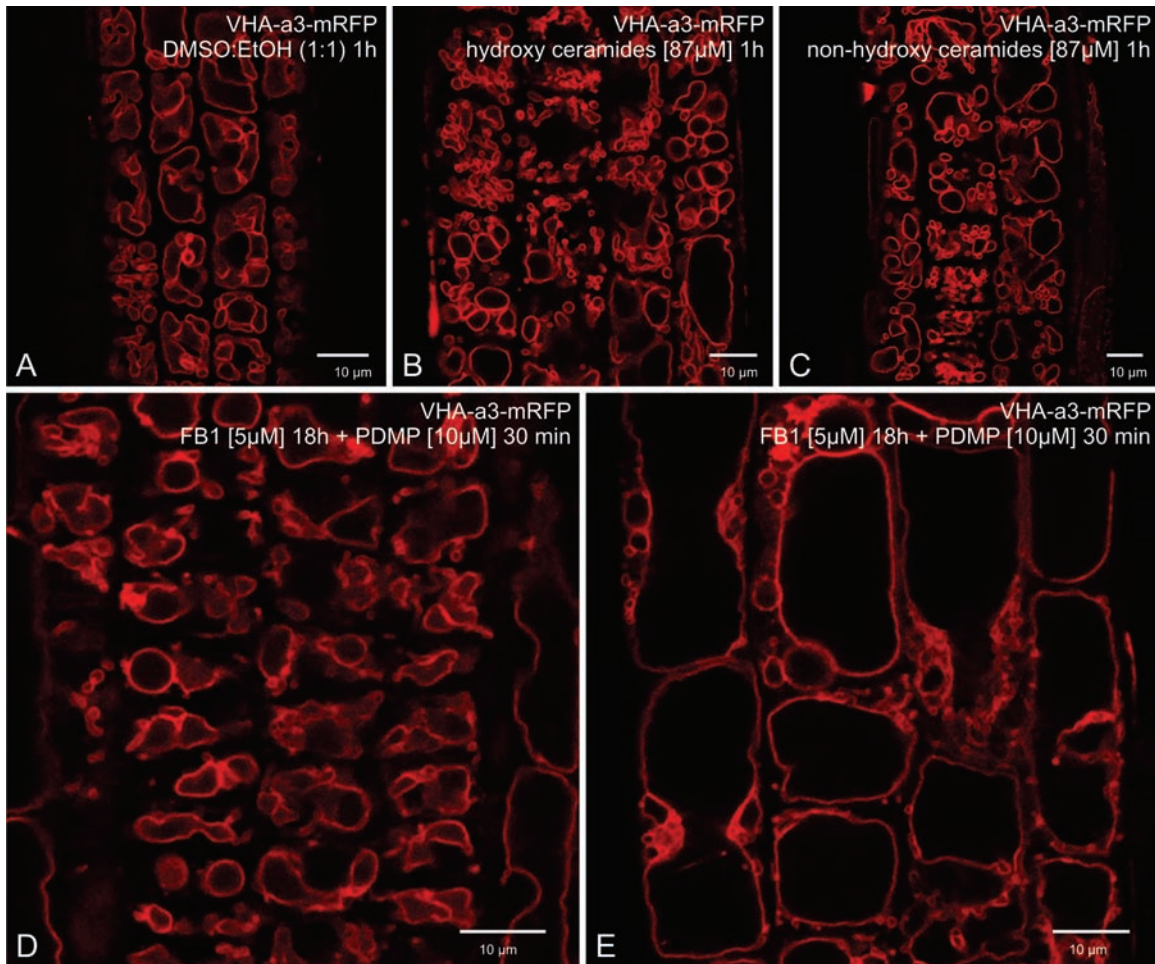
Fig. 6. Attempts to alter ceramide levels in relation to PDMP effects on the vacuole. (A–C) Effects of exposure to exogenously added ceramides for 1 h in comparison to the DMSO/ethanol control (A): larger numbers of smaller vacuoles are present, but vacuolar inclusions are not visible. (D, E) Effect of pretreating cells near the root tip (D) and cells near the elongation zone (E) with the ceramide synthesis inhibitor FB1 (5 µM) before addition of PDMP: vacuolar inclusions were not formed. Bars, 10 µm.

interrupting image acquisition. External ATP was used as a stimulus at the end of each measurement to demonstrate the integrity of the seedlings and responsiveness of the system. Application of 100 µM PDMP perturbed cytoplasmic Ca^{2+} concentrations in *Arabidopsis* roots (Fig. 7A, B). Immediately after applying 100 µM PDMP to the seedlings, cytoplasmic Ca^{2+} concentration gently increased, reaching a peak after 5 min. This was then followed by a slight decrease until a plateau at a higher value than the initial cytoplasmic Ca^{2+} concentration was reached. In contrast, the Ca^{2+} transient triggered by application of 1 mM ATP was much stronger and much faster (Fig. 7B). By comparison, seedlings treated with 10 µM PDMP did not show any detectable change in cytoplasmic Ca^{2+} concentration (Fig. 7C, D). Solvent control treatments (0.1% DMSO) also did not affect cytosolic Ca^{2+} levels (Fig. 7E, F).

Since the Ca^{2+} measurements rely on a fluorescence imaging approach, it is possible to measure parameters such as structural changes on cellular morphology, cell elongation, and cytoplasmic streaming in parallel. Structural changes in cellular morphology were recognizable within seconds after

application of 100 µM PDMP (Fig. 7A and Supplementary Movie S1). The central vacuoles lost turgor pressure and adopted a spherical shape. Moreover, 100 µM PDMP stopped cell elongation although cytoplasmic streaming continued unchanged. Also, the PDMP-induced structural changes and elevating cytoplasmic Ca^{2+} levels were overlapping events and could not be clearly arranged in a temporal order (Supplementary Movie S1). However, none of these effects were in seedlings treated with 10 µM PDMP or in solvent (0.1% DMSO) controls (Fig. 7C, E and Supplementary Movies S2 and S3).

Discussion

Although PDMP is a well-known inhibitor of sphingolipid biosynthesis, both in animals (Futerman and Riezman, 2005) as well as in plants (Melser *et al.*, 2010), it is also recognized as a drug that can induce macroautophagy in mammalian cells. A consequence of PDMP treatment is that cytosolic ceramide levels increase, and this triggers
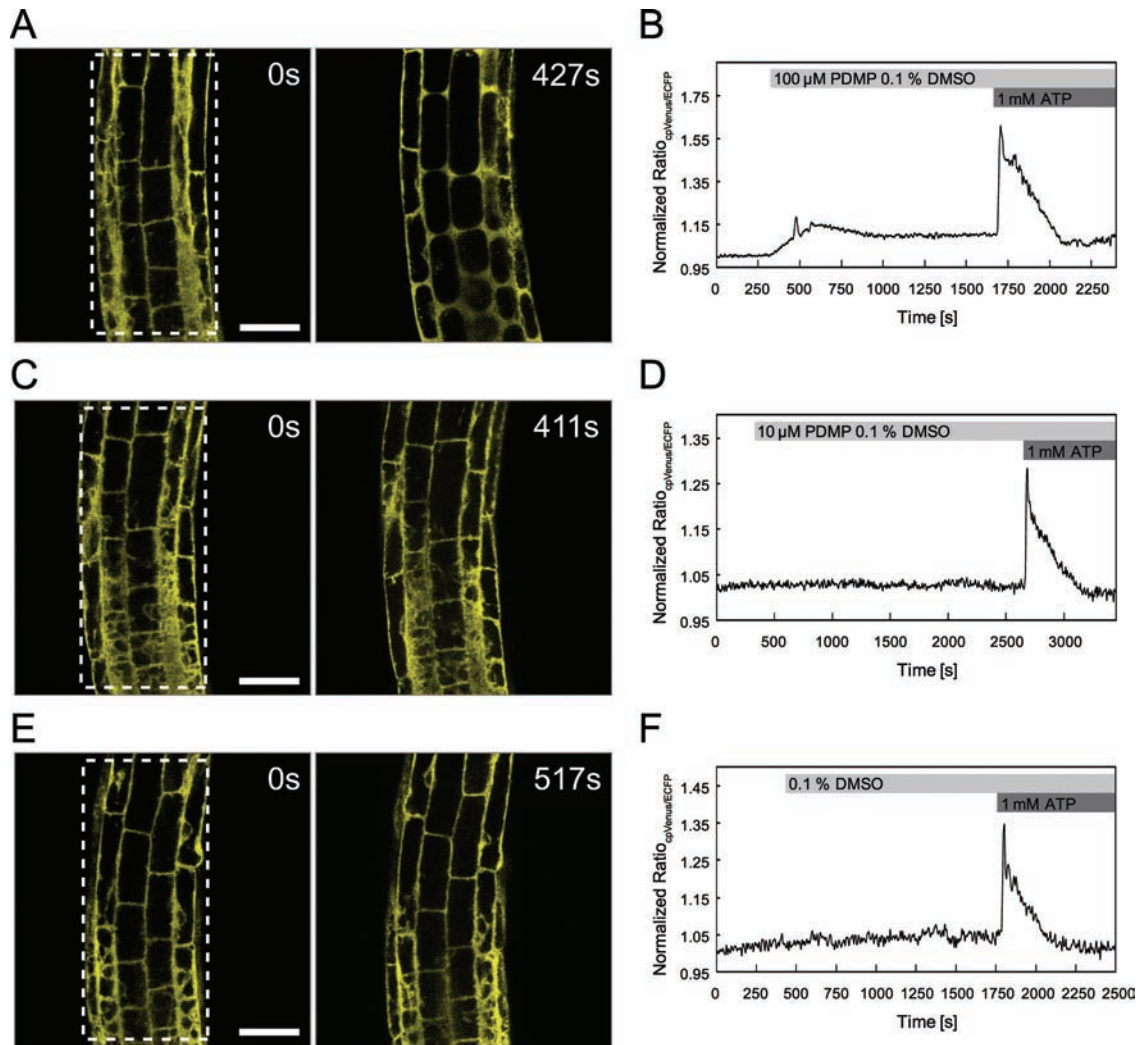
Fig. 7. PDMP- and ATP-induced Ca²⁺ transients in *Arabidopsis* root cells. Ca²⁺ imaging was performed on cortical and epidermal cells of the root elongation zone of *Arabidopsis* seedlings expressing the Ca²⁺ sensor NES-YC3.6. Cytosolic Ca²⁺ dynamics were recorded in defined regions of interests, and the normalized ratio, indicating changes in free cytosolic [Ca²⁺], was monitored over time after application of different treatments. (A, C, E) Fluorescence signal cpVenus at time point zero and 100 s after PDMP/DMSO application. (B, D, F) Normalized emission ratio cpVenus/ECFP. (A, B) A moderate increase in $[Ca^{2+}]_{Cyt}$ was observed after application of 100 µM PDMP, and a more pronounced Ca²⁺ transient was induced by treatment with 1 mM ATP (B); see also Supplementary Movie S1. (C, D) In contrast to application of 1 mM ATP (D), 10 µM PDMP did not induce measurable changes in $[Ca^{2+}]_{Cyt}$; see also Supplementary Movie S2. (E, F) The control treatment (0.1% DMSO) did not affect cytosolic Ca²⁺ levels, whereas 1 mM ATP increased levels of $[Ca^{2+}]_{Cyt}$ (F); see also Supplementary Movie S3. Boxes in A, C, and E indicate the regions of interest for ratiometric measurements. Data are representative of at least three experiments. Data recording was performed every 6 seconds. Bars, 50 µm.

the formation of autophagosomes (Daido *et al.*, 2004; Zeng *et al.*, 2006). Apparently, ceramides interact with two important complexes of the autophagy machinery [mTOR and Beclin1(Atg6)] thus initiating autophagosome formation. However, this effect normally requires much higher PDMP concentrations (100 µM are usual) and longer exposures (of the order of hours) than used in this investigation. Moreover, the data on ConcA together with the observations made on mutant lines lacking different components of the core macroautophagy machinery demonstrate that macroautophagy is not responsible for the formation of PDMP-induced vacuolar inclusions. On the contrary,

careful CLSM analyses of root cells from *Arabidopsis* lines stably expressing tonoplast and endoplasmic reticulum marker proteins have revealed that what superficially appeared to be autophagic bodies are in fact stable tubular invaginations of the tonoplast.

It is known that PDMP has other, non-ceramide-based effects. It has been shown to block brefeldin A-induced retrograde transport of Golgi membranes into the endoplasmic reticulum in mammalian cells (Kok *et al.*, 1998) and also to inhibit anterograde membrane traffic out of the endoplasmic reticulum during brefeldin A recovery (Nakamura *et al.*, 2001). However, PDMP does not

interfere with ARF1 or coatomer binding to Golgi membranes (De Matteis *et al.*, 1999). Instead, it has been shown that these effects of PDMP on the endoplasmic reticulum and Golgi apparatus are due to the release of calcium ions into the cytosol, since the introduction of calcium chelators into the cytoplasm counteracted the PDMP effect (Sprocati *et al.*, 2006). Calcium is released mainly from the endoplasmic reticulum since the endoplasmic reticulum-based Ca^{2+}-ATPase inhibitor thapsigargin reduces considerably the effect of PDMP (Kok *et al.*, 1998), and the release of calcium ions was fast (roughly 1 min after application of PDMP). In contrast to the present observations, the PDMP effect on mammalian cells appeared to be concentration dependent only occurring at 100 µM or higher (Kok *et al.*, 1998). Nevertheless, the present study tested for the possibility that the drastic changes in vacuole morphology might be triggered by a sudden rise in cytosolic calcium. However, while PDMP at a concentration of 10 µM rapidly induces these effects in *Arabidopsis* roots, no change in cytosolic calcium levels were observed at this concentration. Only at 100 µM was an effect of PDMP on cytosolic calcium levels registered, and even then it was much weaker than that induced by ATP application. In addition, structural changes on cellular morphology induced by 100 µM PDMP and the observed cytosolic Ca^{2+} increase take place at the same time. It is therefore concluded that the changes in vacuole morphology induced by 10 µM PDMP in *Arabidopsis* root cells cannot be the result of rapid transient increases in cytoplasmic calcium.

Although it became clear that this study was not dealing with autophagy, it nevertheless attempted to see if the PDMP effects on the vacuole do involve changes in ceramide levels. While exogenously added ceramides do cause morphological changes to the vacuoles in *Arabidopsis* roots, they are not autophagic in character. That ceramides target vacuoles conforms, however, with the fact that programmed cell death, which eventually involves a loss of vacuolar integrity, is induced by ceramides (Dai *et al.*, 2004; Townley *et al.*, 2005). It is known that ceramides can interact with membranes, causing the displacement of sterols from ordered domains (Ramstedt and Slotte, 2006), and can also permeabilize membranes by forming large metastable channels (Anishkin *et al.*, 2006). Thus PDMP, being itself a ceramide analogue, might interdigitate in the lipid bilayer of the tonoplast resulting in vacuolar fusion and residual tonoplast invaginations. However, pretreatment with FB1, which should lead to a decrease in ceramide levels and therefore deprive PDMP of a substrate, seems to prevent the changes induced by PDMP, although some modifications in vacuole morphology were still recorded. It has been reported that FB1 causes the increased presence of 'deconvoluted vacuole-like structures' in *Arabidopsis* root cells (Markham *et al.*, 2011), but it would appear that the principal cytological target for FB1 is the endoplasmic reticulum, at least in tobacco BY-2 cells (Aubert *et al.*, 2011). In conclusion, the results presented here do not exclude the possibility that the PDMP-induced changes in vacuole morphology might still be triggered by increased ceramide levels.

Supplementary material

Supplementary data are available at *JXB* online.

Supplementary Fig. 1. PDMP effects on the Golgi apparatus of *Arabidopsis* root cells.

Supplementary Movie S1. Cytoplasmic Ca^{2+} dynamics in *Arabidopsis* root cells treated with 100 µM PDMP.

Supplementary Movie S2. Cytoplasmic Ca^{2+} dynamics in *Arabidopsis* root cells treated with 10 µM PDMP.

Supplementary Movie S3. Cytoplasmic Ca^{2+} dynamics in *Arabidopsis* root cells treated with 0.1% DMSO.

References

Anishkin A, Sukharev S, Colombini M. 2006. Searching for the molecular arrangement of transmembrane cermide channels. *The Biophysical Journal* **90,** 2414–2426.

Asano N. 2003. Glycosidase inhibitors: update and perspectives on practical use. *Glycobiology* **13,** 93R–104R.

Aubert A, Marion J, Boulogne C, Bourge M, Abreu S, Bellec Y, Faure J-D, Satiat-Jeunemaitre B. 2011. Sphingolipids involvement in plant endomembrane differentiation: the BY2 case. *The Plant Journal* **65,** 958–971.

Bassham DC, Laporte M, Marty F, Moriyasu Y, Ohsumi Y, Olsen LJ, Yoshimoto K. 2006. Autophagy in development and stress responses of plants. *Autophagy* **2,** 2–11.

Brüx A, Liu T-Y, Krebs M, Stierhof Y-D, Lohmann JU, Miersch O, Wasternack C, Schumacher K. 2008. Reduced V-ATPase activity in the trans-Golgi network causes oxylipin-dependent hypocotyl growth inhibition in *Arabidopsis*. *The Plant Cell* **20,** 1088–1100.

Dai Q, Liu JH, Chen J, Durrant D, McIntyre TM, Lee RM. 2004. Mitochondrial ceramide increases in UV-irradiated HeLa cells and is mainly derived from hydrolysis of sphingomyelin. *Oncogene* **23,** 3650–3658.

Daido S, Kanzawa T, Yamamoto A, Takeuchi H, Kondo Y, Kondo S. 2004. Pivotal role of the cell death factor BNIP3 in ceramide-induced autophagic cell death in malignant glioma cells. *Cancer Research* **64,** 4286–4293.

De Matteis MA, Luna A, Di Tullio G, Corda D, Kok JW, Luini A, Egea G. 1999. PDMP blocks the BFA-induced ADP-ribosylation of BARS-50 in isolated Golgi membranes. *FEBS Letters* **459,** 310–312.

Dettmer J, Hong-Hermesdorf A, Stierhof Y-D, Schumacher K. 2006. Vacuolar H+-ATPase activity is required for endocytic and secretory trafficking in *Arabidopsis*. *The Plant Cell* **18,** 715–730.

Futerman AH, Riezman H. 2005. The ins and outs of sphingolipid synthesis. *Trends in Cell Biology* **15,** 312–318.

Guenther GG, Peralta ER, Rosales KR, Wong SY, Siskind LJ, Edinger AL. 2008. Ceramide starves cells to death by

downregulating nutrient transporter proteins. *Proceedings of the National Academy of Sciences, USA* **105,** 17402–17407.

Hillmer S, Viotti C, Robinson DG. 2012 An improved procedure for low-temperature embedding of high-pressure frozen and freeze-substituted plant tissues resulting in excellent structural preservation and contrast. *Journal of Microscopy* **247,** 43–47.

Hofius D, Schultz-Larsen T, Joensen J, Tsitsigiannis DI, Petersen NHT, Mattsson O, Jorgensen LB, Jones JDG, Mundy J, Petersen M. 2009. Autophagic components contribute to hypersensitive cell death in *Arabidopsis*. *Cell* **137,** 773–783.

Inoue Y, Suzuki T, Hattori M, Yoshimoto K, Ohsumi Y, Moriyasu Y. 2006. AtATG genes, homologs of yeast autophagy genes, are involved in constitutive autophagy in *Arabidopsis* root tip cells. *Plant and Cell Physiology* **47,** 1641–1652.

Kok JW, Babia T, Filipeanu CM, Nelemans A, Egea G, Hoekstra D. 1998. PDMP blocks brefeldin A-induced retrograde membrane transport from Golgi to ER: evidence for involvement of calcium homeostasis and dissociation from sphingolipid metabolism. *Journal of Cell Biology* **142,** 25–38.

Krebs M, Held K, Binder A, Hashimoto K, Den Herder G, Parniske M, Kudla J, Schumacher K. 2012. FRET-based genetically encoded sensors allow high-resolution live cell imaging of Ca2+ dynamics. *The Plant Journal* **69,** 181–192.

Kwon IS, Park OK. 2008. Autophagy in Plants. *Journal of Plant Biology* **51,** 313–320.

Li F, Vierstra RD. 2012. Autophagy: a multifaceted intracellular system for bulk and selective recycling. *Trends in Plant Science* **8,** 982–984.

Liang H, Yao N, Song LT, Luo S, Lu H, Greenberg LT. 2003. Ceramides modulate programmed cell death in plants. *Genes and Development* **17,** 2636–2641.

Markham JE, Molino D, Gissot L, Bellec Y, Hématy K, Marion J, Belcram K, Palauqui J-C, Satiat-JeuneMaitre Ba, Faure J-D. 2011. Sphingolipids containing very-long-chain fatty acids define a secretory pathway for specific polar plasma membrane protein targeting in *Arabidopsis*. *The Plant Cell* **23,** 2362–2378.

Melser S, Batailler B, Peypelut M, Poujol C, Bellec Y, Wattelet-Boyer V, Maneta-Peyret L, Faure J-D, Moreau P. 2010. Glucosylceramide biosynthesis is involved in golgi morphology and protein secretion in plant cells. *Traffic* **11,** 479–490.

Nakamura M, Kuroiwa N, Kono Y, Takatsuki A. 2001. Glucosylceramide synthesis inhibitors block pharmacologically induced dispersal of the Golgi and anterograde membrane flow from the endoplasmic reticulum: implication of sphingolipid metabolism in maintenance of the Golgi architecture and anterograde membrane flow. *Bioscience, Biotechnology and Biochemistry* **65,** 1369–1378.

Neubert C, Graham LA, Black-Maier EW, Coonrod EM, Liu T-Y, Stierhof Y-D, Seidel T, Stevens TH, Schumacher K. 2008. *Arabidopsis* has two functional orthologs of the yeast V-ATPase assembly factor Vma21p. *Traffic* **9,** 1618–1628.

Ramstedt B, Slotte JP. 2006. Sphingolipids and the formation of sterol-enriched ordered membrane domains. *Biochimica et Biophysica Acta* **1758,** 1945–1956.

Ritzenthaler C, Nebenfuhr A, Movafeghi A, Stussi-Garaud C, Behnia L, Pimpl P, Staehelin LA, Robinson DG. 2002. Reevaluation of the effects of brefeldin A on plant cells using tobacco bright yellow 2 cells expressing Golgi-targeted green fluorescent protein and COPI antisera. *The Plant Cell* **14,** 237–261.

Scheuring D, Viotti C, Krueger F, *et al.* 2011. Multivesicular bodies mature from the trans-Golgi network/early endosome in *Arabidopsis*. *The Plant Cell* **23,** 3463–3481.

Spassieva SD, Markham JE, Hille J. 2002. The plant disease resistance gene Asc-1 prevents disruption of sphingolipid metabolism during AAL-toxin-induced programmed cell death. *The Plant Journal* **32,** 561–572.

Sprocati T, Ronchi P, Raimondi A, Francolini M, Borgese N. 2006. Dynamic and reversible restructuring of the ER induced by PDMP in cultured cells. *Journal of Cell Science* **119,** 3249–3260.

Thompson AR, Doelling JH, Suttangkakul A, Vierstra RD. 2005. Autophagic nutrient recycling in *Arabidopsis* directed by the ATG8 and ATG12 conjugation pathways. *Plant Physiology* **138,** 2097–2110.

Townley HE, McDonald K, Jenkins GI, Knight MR, Leaver CJ. 2005. Ceramides induce programmed cell death in *Arabidopsis* cells in a calcium-dependent manner. *Biological Chemistry* **386,** 161–166.

Viotti C, Bubeck J, Stierhof Y-D, *et al.* 2010. Endocytic and secretory traffic in *Arabidopsis* merge in the trans-Golgi network/early endosome, an independent and highly dynamic organelle. *The Plant Cell* **22,** 1344–1357.

Vunnam RR, Radin NS. 1980. Analogs of ceramide that inhibit glucocerebroside synthetase in mouse brain. *Chemistry and Physics of Lipids* **26,** 265–278.

Yoshimoto K, Hanaoka H, Sato S, Kato T, Tabata S, Noda T, Ohsumi Y. 2004. Processing of ATG8s, ubiquitin-like proteins, and their deconjugation by ATG4s are essential for plant autophagy. *The Plant Cell* **16,** 2967–2983.

Zeng XH, Overmeyer JH, Maltese WA. 2006. Functional specificity of the mammalian Beclin-Vps34 PI 3-kinase complex in macroautophagy versus endocytosis and lysosomal enzyme trafficking. *Journal of Cell Science* **119,** 259–270.